Egypt. J. Chem. **Vol.68** , No.8 pp.147 - 159 (2025)

Egyptian Journal of Chemistry

http://ejchem.journals.ekb.eg/

Green corrosion inhibition of carbon steel by expired sulfaquinoxalineq drug in 1 M HCl medium: A comprehensive study

Mahmoud A. Ali[1], Ahmed A. El-Hossiany[1,2], Abdelfattah M. Ouf[1], Mohamed E. Elgamil[3], Abd El-Aziz S. Fouda[1*]

[1] *Department of Chemistry, Faculty of Science, Mansoura University, Mansoura-35516, Egypt, Tel: +2 050 2365730, Fax: +2 050 2202264*

[2] *Delta for Fertilizers and Chemical Industries, Talkha-1179, Egypt.*

[3] *Higher Institute of Engineering and Technology, Tanta, Egypt.*

Abstract

Expired Sulfaquinoxalineq drug (ESD) was used as a green corrosion inhibitor for carbon steel (CS) in 1.0 M HCl. There are many techniques used in this study to explain the inhibition process. The first technique is WL technique which used to measure the inhibition productivity of ESD on CS. The second technique is electro chemical techniques which contains (Tafel polarization (TP), and electrochemical impedance spectroscopy (EIS)). The third technique is surface examination technique to conform the protective film formation and it contains atomic force microscopy (AFM), and the FT-IR spectroscopy. The study revealed a direct correlation between the concentration of the drug and its inhibitory effect on corrosion. As the drug concentration rose from 50 to 300 ppm, the inhibition efficiency (IE) steadily improved. The highest IE of 93.2% was achieved at a drug concentration of 300 ppm, both in the case of WL and EIS. The findings suggest that the drug acts as a mixed-type inhibitor. EIS spectra displayed a single capacitive loop, indicating that the corrosion process is primarily controlled by charge transfer. To elucidate the inhibition mechanism, the activation energy (E^*_a) and several thermodynamic parameters were calculated. These included the adsorption equilibrium constant (K_{ads}), free energy of adsorption (ΔG^o_{ads}), adsorption enthalpy (ΔH^o_{ads}), and adsorption entropy (ΔS^o_{ads}). The adsorption of ESD followed the Langmuir adsorption isotherm. Quantum chemical calculations were performed and analyzed, providing support for the experimental findings. The predicted corrosion efficiencies of these compounds closely aligned with the experimental measurements.

Keywords: Corrosion inhibition, Carbon steel, HCl, Langmuir isotherm, Quantum chemical calculatio

1. Introduction

The corrosion of the metal is one of the most popular problems in many industrial applications. It is occurred due to the interaction between metal and the surround medium [1]. To overcome those problems, we use inhibitor to reduce the metal corrosion and make the metal more effective [2]. "CS is one of the metals which used in industrial applications and they corroded when used in acidic solutions such acid HCl solutions [3]. In industrial field we use the acidic solution in numerous uses such as acid pickling; acid rescaling and petrochemical processes [4]. Plant extract is the most applicable inhibitor which used to reduce the metal corrosion because it is not expensive and not have a harmful effect on the environment [5]. Expired drugs, due to their low cost and minimal environmental impact, are increasingly explored as green corrosion inhibitors for metals and alloys. Most well-known acid drugs are organic compounds containing nitrogen (N-heterocyclic), sulfur, long carbon chain or aromatic and oxygen atoms. Among them, drugs have many advantages such as: high molecular size, highly soluble in water, availability, low price, low toxicity, and easy production [7]**.** Organic heterocyclic compounds have been used for the corrosion inhibition of carbon steel [8], copper [9], aluminum [10]**,** and other metals [11] in different aqueous media. Adsorption of the drug molecules on the metal surface facilitates its inhibition [12]. A few medications have been discovered to be great corrosion inhibitors for metals such as: Biopolymer gave 86% IE for Cu in NaCl [13], pyromellitic diimide linked to oxadiazole cycle gave 84.6% IE for CS in HCl [14], 2-mercaptobenzimidazole gave 82% IE for CS in HCl [15], Antidiabetic drug Janumet gave 88.7% IE for mild steel in HCl [16], Januvia gave 79.5% IE for Zn in HCl [17], Cefuroxime Axetil gave 89.9% IE for Al in HCl [18], Phenytoin sodium gave 79% for CS in HCl [19], Aspirin gave71% IE for mild steel in H_2SO_4 [20], Septazole gave 84.8% IE for Cu in HCl [21] and Chloroquine diphosphate gave 80% IE for mild steel in HCl [22]. While considerable research has focused on utilizing drugs as corrosion inhibitors for metals, the application of expired drugs in this context remains relatively unexplored.

*Corresponding author e-mail: asfouda@hotmail.com (Abdelaziz Fouda)
Received Date: 28 September 2024, Revised Date: 05 December 2024, Accepted Date: 23 December
DOI:10.21608/EJCHEM.2024.324472.10535

This study introduces a novel approach to repurposing expired Sulfaquinoxalineq as a corrosion inhibitor for carbon steel in 1M HCl medium. The choice of use of ESD because of it contains N (N-heterocyclic), Oxygen, long carbon series and aromatic composite, that utilized in the process of protecting the metals as well as cheapness and availability". In this research, several studies have been utilized to examine the protection behavior, including TP, EIS and WL studies, in addition to studying the metal surface by numerous techniques.

2. Experimental techniques

2.1. CS sample

Table 1: Represented the concentration of the elements which present in CS

wt. %	C	Si	Mn	S	P	Fe
CS	0.20	0.003	0.35	0.025	0.02	the rest

2.2. Chemicals

Sulfaquinoxalineq drug is an organic composite, which have the chemical formula $C_{24}H_{20}N_6O_3$ and purchased from Sandozinc and Pfizer inc. companies was utilized here as inhibitor

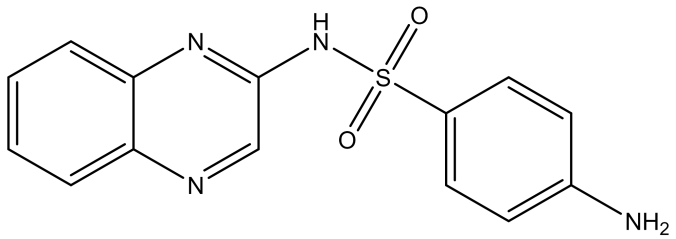

4-amino-N-(quinoxalin-2-yl) benzene sulfonamide
Chemical Formula: $C_{14}H_{12}N_4O_2S$, Molecular Weight: 300.34

A wide variety of sulfonamides are used to treat bacterial infections and to prevent coccidiosis.
Sulfaquinoxalineq is used as an adjunct in some anticoagulant rodenticide products. Additionally, several of the sulfonamides are combined with trimethoprim to produce the potentiated sulfonamides that exhibit a broader antibacterial spectrum [23].

2.3. Solutions

The corrosive environment is 1.0 M HCl which ready by using double distilled water and using stock of 37% HCl (purchased from El-Nasr, Egypt) then it standardized using Na_2CO_3. A stock solution of ESD was prepared (1000 ml) by weighing one gram of the drug and dissolved it in one liter of doubly distilled water and from this stock solution, the used concentrations (50,100,150,200,250,300 ppm) were prepared by dilution.

2.4. The list of methods which used to calculate % IE

2.4.1 WL method

For the weight loss study, the carbon steel specimens were prepared according to ASTM G31-72 standards [24]. "This method was used to detect the IE of ESD when applied to CS in 1 M HCl. The size of CS pieces was (2 cm x 2cm x 0.2 cm). Carbon steel coupons were abraded with emery paper of varying grit grades (600-2000), rinsed with distilled water, dried, and weighed (W1). The coupons were then suspended in 100 mL beakers using glass hooks. Corrosive solutions with and without varying concentrations of the drug were introduced into the beakers. After a specified duration, the coupons were removed, washed with distilled water and acetone, dried, and weighed (W_2). Weight loss (ΔW) was calculated as the difference between the initial (W_1) and final (W_2) weights".

The inhibition efficiency (% IE) and surface coverage area (θ) were determined using Eq. 1[25]:

$$\% IE = \theta \times 100 = [1 - (\Delta W / \Delta W^o)] \times 100 \quad (1)$$

Where, ΔW^o and ΔW are the WL in presence and absence of various doses of the ESD. The corrosion rate equation is given by:

$$k_{corr} = (\Delta W / A) / (\rho t) \quad (2)$$

where: ΔW = weight loss (mg), A = surface area of the specimen (cm²), ρ = density of the metal (g/cm³), t = time of exposure (min)

This equation calculates the corrosion rate based on the weight loss of a metal specimen over a given time period.

2.4.2. Electrochemical measurements

There are two techniques were applied in electrochemical measurements (EIS, TP). "This study performed at 25°C by using laboratory instrument (Gamry (PCI4/750) Potentiostat/ Galvanostat/ZRA) and electrodes cell which contain three electrodes. Emery paper was used to polish the working electrode before starting any technique [26]. TP technique was applied by changeable the potential of electrode from -800 to 200 mV with a scan rate of 0.2 mV/s. EIS was performed using AC signals and the frequency range was (0.01- 100,000 Hz) at 10 mV". The % IE was determined as next for TP methods:

$$\% IE_{EFM} = 100 \times [1 - (i_{corr.} / i^o_{corr.})] \quad (3)$$

Where, i^o_{corr} and i_{corr} are the current densities without and with ESD.

2.5. Surface Analysis

2.5.1 Atomic force microscopy (AFM) technique

The technique you're describing is AFM, specifically using the Pico SPM2100 AFM device. AFM is a powerful tool for studying surfaces at an atomic level.

2.5.2. Attenuated total reflection Fourier-transform infrared *(*ATR-FTIR*)* spectroscopy

FT-IR spectra were acquired using a Thermo Fisher Scientific instrument in Waltham, MA, USA. "These spectra provided information about the inhibitor's molecular structure through the identification of peaks associated with specific functional groups within the inhibitor's chemical composition".

3. Results and discussion

3.1. WL tests

Figure 1 illustrates the weight loss (WL) curves for carbon steel (CS) immersed in 1M HCl solution both with and without the presence of electrostatic discharge (ESD). "Using these curves, we calculated the corrosion rate (kcorr), inhibition efficiency (%), and activation energy (Θ) for CS at various temperatures ranging from 25°C to 45°C [27]. The obtained data is summarized in Table 2. The table reveals a clear trend: increasing the dose of ESD leads to an increase in inhibition efficiency, while the corrosion rate rises with increasing temperature. [28]. This phenomenon is caused by the adsorption of the active molecules of the drug on the CS surface. The maximum IE of 93.2 % was obtained at 300 mg/L drug dose". k_{corr} increases as the immersion period is lengthen at a fixed dose of the drug and with rise in temperature.

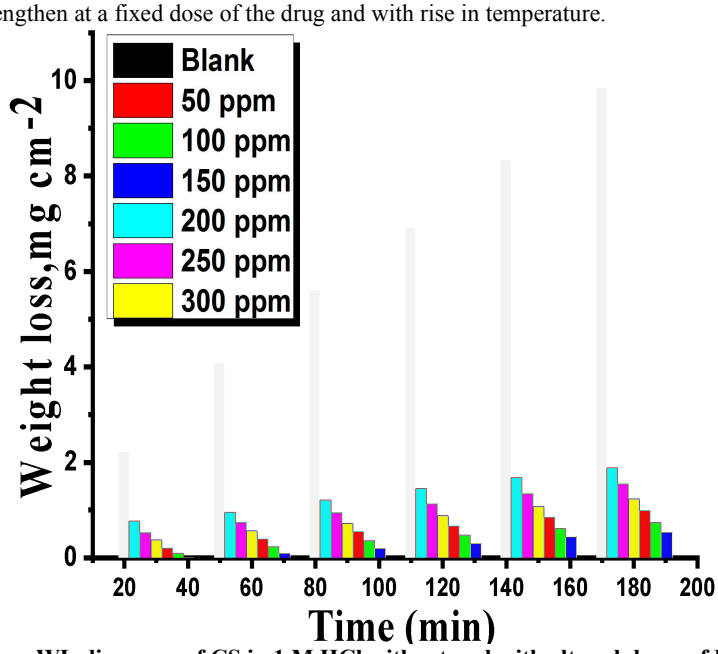

Fig. 1. Time *vs.* WL diagrams of CS in 1 M HCl without and with altered doses of ESD at 25° C

Table 2: Outcome data of WL measurements of CS at temperatures (25-45°C) at 120 min dipping in the attendance and lack of altered doses of ESD

Temp., °C	[inh], ppm	k_{corr}, mg cm^{-2} min^{-1}	Θ	% IE
25	Blank	0.069±0.0017	----	----
	50	0.0077±0.0015	0.888	88.8
	100	0.0067±0.0013	0.903	90.3
	150	0.0062±0.0010	0.910	91.0
	200	0.0057±0.0012	0.917	91.7
	250	0.0051±0.0019	0.926	92.6
	300	0.0047±0.0018	0.932	93.2
30	Blank	0.087±0.0021	----	----
		0.0108±0.0020	0.876	87.6
	100	0.0101±0.00012	0.884	88.4
	150	0.0093±0.00013	0.893	89.3
	200	0.0084±0.00014	0.903	90.3
	250	0.0077±0.00017	0.911	91.1
	300	0.0066±0.00016	0.924	92.4
	Blank	0.11±0.00018	----	----

35	50	0.0188±0.00015	0.829	82.9
	100	0.0175±0.00014	0.841	84.1
	150	0.0159±0.00016	0.855	85.5
	200	0.0143±0.00010	0.870	87.0
	250	0.0132±0.00011	0.880	88.0
	300	0.0118±0.00014	0.893	89.3
40	Blank	0.155±0.00017	----	----
	50	0.029±0.00015	0.813	81.3
	100	0.0264±0.00016	0.830	83.0
	150	0.0245±0.00014	0.842	84.2
	200	0.0232±0.00018	0.850	85.0
	250	0.0211±0.00019	0.864	86.4
	300	0.0181±0.00021	0.883	88.3
45	Blank	0.177±0.00012	----	----
	50	0.0345±0.00017	0.805	80.5
	100	0.0317±0.00018	0.821	82.1
	150	0.0306±0.00019	0.827	82.7
	200	0.0281±0.00018	0.841	84.1
	250	0.0252±0.00012	0.858	85.8
	300	0.0214±0.00022	0.879	87.9

3.1.1Adsorption isotherms

The weight loss data was used to construct a Langmuir adsorption isotherm, "which allowed for the calculation of thermodynamic parameters. Eq.3 was used to explain Langmuir isotherm and from it we plot the linear relation among C/Θ and C with slope nearly unit (Fig. 2) and drug particles cover a monolayer on the CS surface [29,30]. ΔG^0_{ads} and K_{ads} (adsorption parameters) calculated by using (Eq. 4)" [31].

$$C/\Theta = 1/K_{ads} + C \qquad (3)$$

$$\Delta G^o_{ads} = RT \ln (K_{ads} \times 55.5) \qquad (4)$$

"Table 3 presents the values of $\Delta G°_{ads}$ (standard Gibbs free energy of adsorption) as a function of temperature, averaged over the range of 298-318 K. The $\Delta H°_{ads}$ (standard enthalpy of adsorption) value was determined using the Van't Hoff equation":

$$\log K_{ads} = \frac{-\Delta H^o_{ads}}{2.303RT} + constant \qquad (5)$$

"A linear relationship was observed when plotting log K_{ads} against 1/T (Figure 3). The slope of this line allowed for the determination of ΔH°ads. By combining the calculated values of $\Delta G°_{ads}$ and $\Delta H°_{ads}$, the entropy of adsorption ($\Delta S°_{ads}$) was determined at all investigated temperatures."

$$\Delta S^o_{ads} = \frac{\Delta H^o_{ads} - \Delta G^o_{ads}}{T} \qquad (6)$$

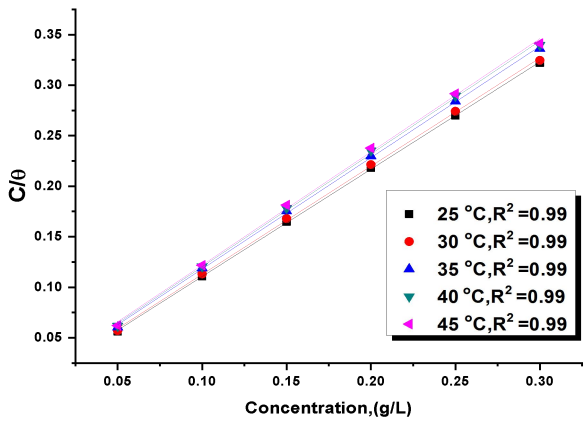

Fig. 2. Curves of Langmuir adsorption of CS without and attendance altered doses of ESD

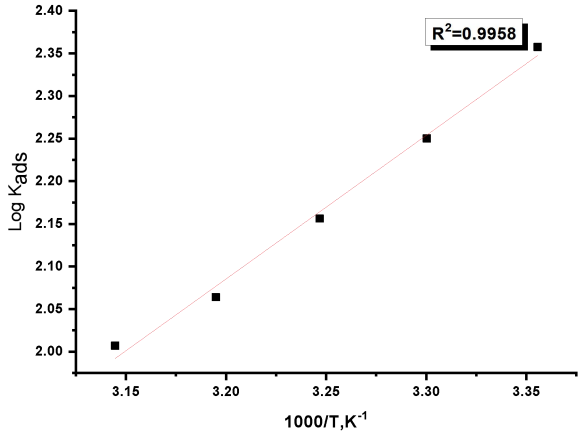

Fig. 3. plot of log K_{ads} vs 1/T for the adsorption of ESD on CS in 1M HCl

Table 3: Langmuir parameters of ESD on CS surface by Langmuir isotherm

Temp. °C	K_{ads} M^{-1}	$-\Delta G^{o}_{ads}$ kJ mol^{-1}	$-\Delta H^{o}_{ads}$ kJ mol^{-1}	ΔS^{o}_{ads}- J $mol^{-1}K^{-1}$
25	227	23.4		29.6
30	177	23.2	32.3	29.9
35	146	23.1		31.1
40	115	22.8		30.3
45	97	22.7		30.8

From (Table 3) we noted that:

1. The adsorption parameters ΔG°ads and K_{ads} were found to increase with increasing temperature.
2. The negative value of ΔG°ads indicates that the adsorption process is spontaneous.
3. The ΔG°ads values, "approximately 20 kJ mol-1, suggest that the drug is physically adsorbed onto the carbon steel surface" [31].
4. "The negative sign of ΔH°ads indicates an exothermic adsorption process [32,33], suggesting either physical or chemical adsorption of the drug onto the carbon steel surface".

3.1.2. Activation parameters

"Activation parameters were employed to elucidate the reaction mechanism between electrostatic discharge (ESD) and the carbon steel (CS) surface. The Arrhenius and transition state equations (Equations 7 and 8) were utilized to interpret this mechanism".

$$k_{corr} = A\, e^{-E^{*}a/RT} \quad (7)$$

$$k_{corr} = RT/Nh\, e^{(\Delta S^{*}/R)}\, e^{(-\Delta H^{*}/RT)} \quad (8)$$

Ea, ΔH*, and ΔS* represent the activation energy, enthalpy, and entropy, respectively. "These kinetic parameters can be determined by plotting log kcorr against 1/T (Figure 4), which yields a straight line [34]. The slope of this line provides the activation energy (Ea). To obtain the values of ΔH* and ΔS*, a linear relationship between log kcorr/T and 1/T is plotted (Figure 5). From this plot, these parameters can be calculated". The activation data are recorded in (Table 4) which explained that":

1. "The adsorption of ESD onto the carbon steel (CS) surface forms a physical barrier, which reduces corrosion and increases the energy barrier for the corrosion process. As a result, the activation energy (Ea) values are higher in the presence of ESD compared to its absence".
2. The positive ΔH* value indicates the presence of an endothermic reaction.
3. The negative ΔS* value suggests that the activated complex at the rate-determining step favors association or coagulation rather than dissociation in solution [35].

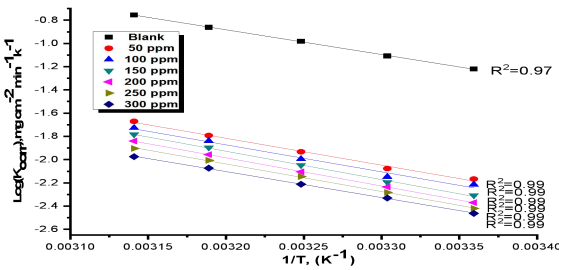

Fig.4. log k_{corr} vs 1/ T for CS in with and without ESD in 1M HCl

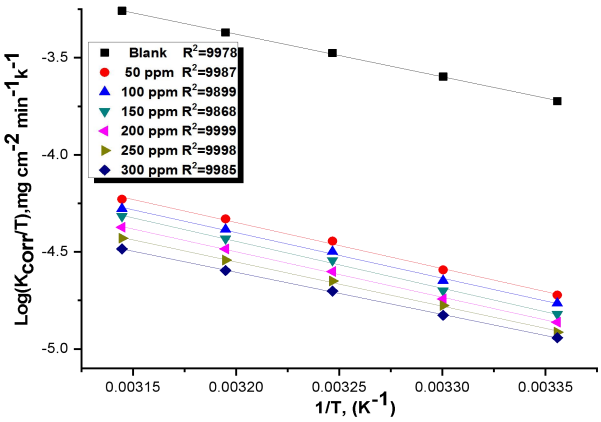

Fig. 5. log k_{corr} / T vs 1/ T for CS without and with ESD in 1M HCl

Table 4: Activation parameters of CS in presence and absence of ESD in 1M HCl

Conc. ppm	E^*_a, kJ mol^{-1}	ΔH^*, kJ mol^{-1}	$-\Delta S^*$, J mol^{-1}K^{-1}
1 M HCl	39.9	37.3	137.1
50	58.6	56.0	75.3
100	59.9	57.3	72.5
150	62.1	59.5	61.6
200	65.4	62.8	57.9
250	66.2	63.6	55.4
300	66.9	64.3	54.5

3.2. Open potential circuit (OCP) measurements

It is necessary to measure the variation of OCP with time for the working electrode before any corrosion rate measurements. "Such step is very significant in setting fields of corrosion, partial and complete inhibition. Fig. 6 shows the variation of OCP as function of time for CS in 1 M HCl solution in the presence and absence of investigated inhibitor at varying concentrations at 298 K. The Figure shows the attainment of a constant potential after about 400 sec of immersion which corresponds to the free corrosion of CS in 1 M HCl solution. It is obviously noted that the potential of CS was shifted to more noble (less negative) values upon addition the altered concentrations from 150 to 300 ppm. Such positive shift of the steady state potential suggests the capability of the investigated inhibitors to retard the corrosion of CS in acidic medium and their influence on the anodic process".

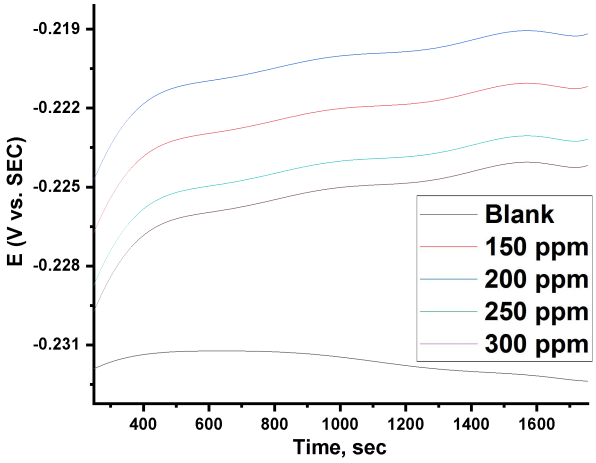

Fig. 6. Changes in E_{OCP} vs. time for CS in the 1.0 M HCl either alone or with various dosages of inhibitor at 298 K

3.3. EIS method

Determine of CS corrosion inhibition detected by studying electrochemical frequency modulation technique in existence and lack of various doses of ESD. "EIS technique was performed in the frequency range (10 kHz t- 10 mHz) at 25°C.This technique described by two Figs. 7 & 8, where Fig. 7 represented the Nyquist plots and Fig. 8 represented the bode plots .The diagram of the Nyquist plots is semicircle and its diameter improved by raising the dose of ESD and the bode plots are open circle curves [36]. The Nyquist bends were examined by fitting the outcome data to an equivalent circuit Fig. 9. EIS parameters R_{ct} (charge transfer resistance), C_{dl} (capacitance double layer), Θ (surface coverage area), IE (inhibition efficiency)", are recorded in Table 5. IE detected by using Eq. 9:

$$\% \text{ IE} = R_{ct} - R_{ct0} / R_{ct} \times 100 \qquad (9)$$

"Where R_{ct} and R_{ct0} are charge transfer resistance in attendance and lack of ESD. By improving the ESD concentration, the data of R_{ct} and IE% raised but the value of the C_{dl} decreased". The outcomes are related to the increasing in double electric and lowering in local dielectric constant [37].

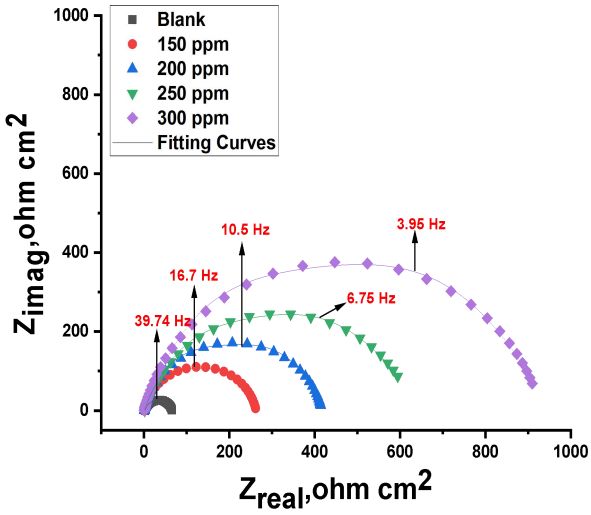

Fig. 7. Nyquist diagram of CS with and without altered doses of ESD in 1M HCl

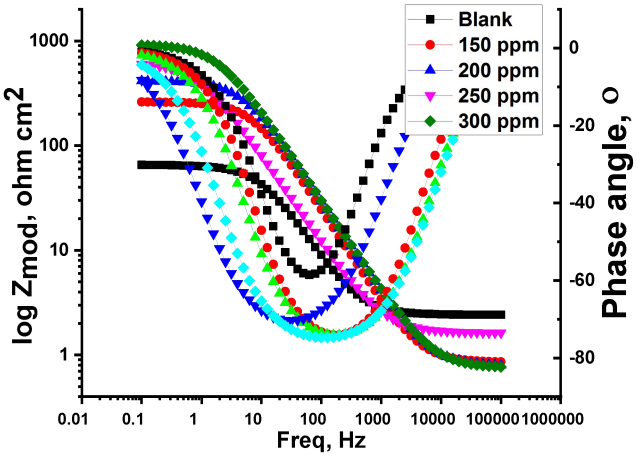

Fig. 8. Bode diagram for CS dissolution attendance and lack altered doses of ESD

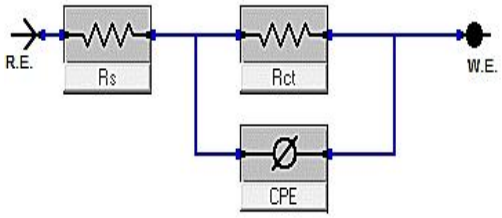

Fig. 9. Simple circuit utilized to fit the EIS outcomes

Table 5: EIS parameters of CS with and without various doses of ESD in 1 M HCl

[Inh] ppm	n	Y_o, ($\mu\Omega^{-1}$ s^n cm^{-2})	R_{ct} Ω cm^2	C_{dl} μFcm^{-2}	θ	%IE	Goodness of fit ($\chi 2$)
Blank	0.879	418	63	253	----	----	$19.78x10^{-3}$
150	0.871	226	261	148	0.759	75.9	$21.57x10^{-3}$
200	0.868	188	416	127	0.849	84.9	$20.78x10^{-3}$
250	0.849	167	628	111	0.900	90.0	$17.89x10^{-3}$
300	0.845	136	929	93	0.932	93.2	$20.14x10^{-3}$

3.4. TP tests

Electrochemical study of corrosion of CS surface in 1 M HCl in existence and nonexistence of altered ESD doses of was achieved by using potentiodynamic polarization study which showed by Fig. (10). "TP parameters like as (I_{corr}, E_{corr}, bc, ba, IE, and θ) are recorded in Table 6.From the table we noted that: 1)i_{corr} decreased by increasing the concentration of ESD. 2) Values of β_c and β_a are changed slightly which improve the effectiveness of ESD on the cathodic and anodic reactions. 3) By raising the dose of ESD the data of θ and IE increased. 4) E_{corr} changed slightly to the cathodic and anodic direction which improved that the cathodic and anodic reactions were protected and ESD acts as mixed type inhibitor" [38]. % IE was measured from Eq. 2:

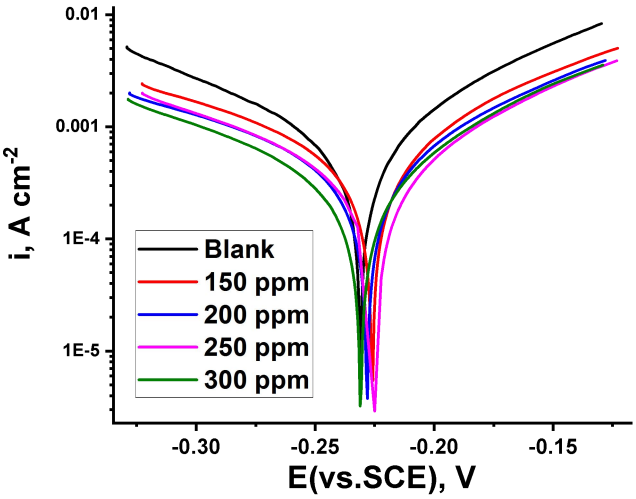

Fig.10. TP of CS dissolution in the attendance and absence of ESD in 1M HCl

Table 6: TP parameters of CS in dissimilar doses of ESD

Conc., mol L^{-1}	$-E_{corr}$, mV (mVvs.SCE),	β_a, mV dec^{-1}	$-\beta_c$, mV dec^{-1}	i_{corr}, μA m^{-2}	θ	% IE_{PDP}
Blank	231	99	156	1080	----	----
150	226	98	186	201	0.814	81.4
200	228	123	250	187	0.827	82.7
250	224	91	135	121	0.888	88.8
300	231	109	185	93	0.914	91.4

3.5. Surface examination

3.5.1. AFM study

AFM is one the most powerful method which used to detect the effect of ESD on CS surface by studying the morphology of the surface. "CS surface was prepared before starting this examination by polishing its surface and immersion of CS pieces in HCl solution for 24 hrs in existence and nonexistence of 300 ppm ESD [39]. Topographic maps of CS surface are represented in Fig. 11 where 2D and 3D images were appeared. Table 7 contains AFM data such as (Rq (square roughness) and Ra (average roughness). Ra has a small value in case of free CS and its value is high in case of CS in HCl solution, but it decreased with the addition of ESD".

Table 7: AFM data for CS surface

Specimen	CS in 1 M HCl	CS in presence of ESD
Rq (nm)	463	154
Ra (nm)	378	124

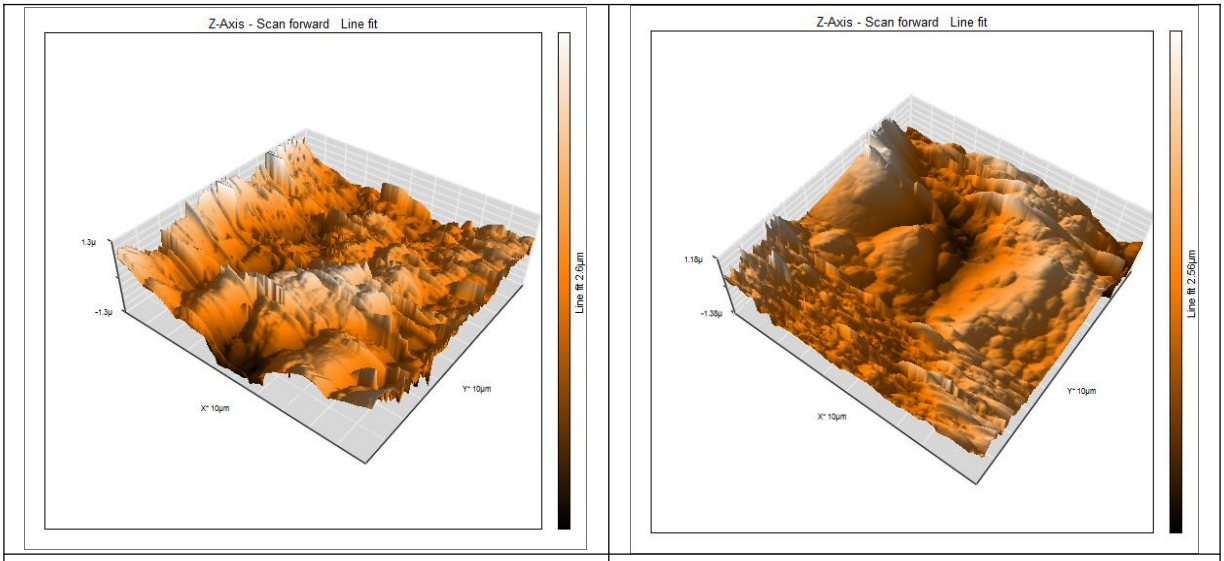

a-Blank **b-ESD**

Fig. 11. AFM (2D and 3D) of CS surface in existence of ESD in 1M HCl

3.5.2. ATR-FTIR Analysis

FTIR analysis was conducted to investigate potential interactions between the adsorbed inhibitor molecules and the carbon steel surface in the acidic environment. "FTIR spectra provide valuable information about the functional groups present in the inhibitor molecules that are adsorbed onto the metal surface. Figure 12 compares the FTIR spectra of pure ESD and ESD adsorbed on the carbon steel surface. Each peak has a certain value on the spectra to facilitate the definition of the effective groups. It is also utilized for determine the type of reaction between CS surface and ESD [40]. CS specimens were prepared before starting the study by polishing it and then immersion in 1M HCl solution in attendance and lack of ESD for 6 hr. Fig. (12) shows certain peaks which define the functional groups of the ESD. There are many bands which appeared on the spectra such as: The broad band appeared at 3385 cm-1 which detect (OH) ,the band appeared at 1635 cm-1 which detect (C=C) and the sharp band at 1015 cm-1 corresponds to (C-O)". There is a small shift in some functional groups indicating the interaction between the CS and ESD [40].

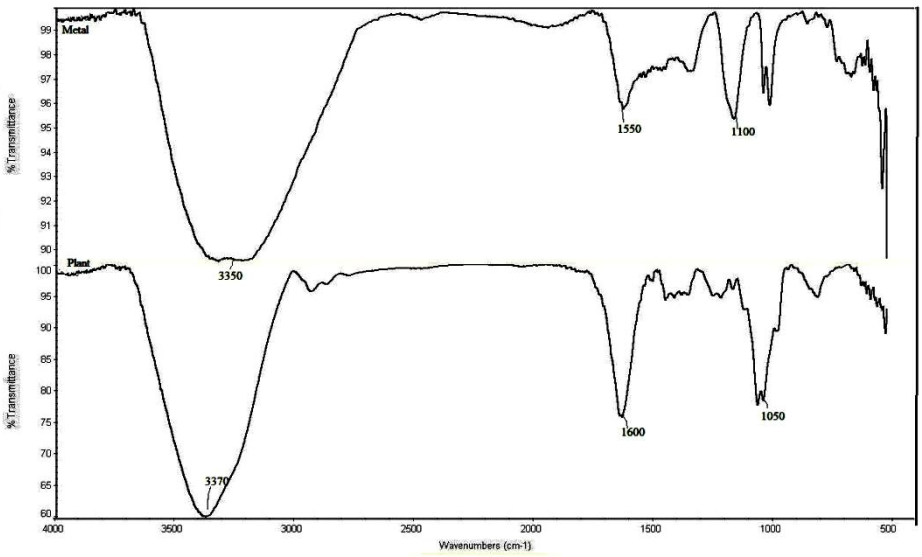

Fig. 12. ATR- FTIR spectra of CS in existence and nonexistence of ESD

3.6. Quantum chemical calculation

Figure 13 presents the frontier molecular orbitals (HOMO and LUMO) for the molecule. "Density Functional Theory (DFT) calculations were performed to determine the molecule's electron density distribution and quantum chemical properties. These properties, including the highest occupied molecular orbital (E_{HOMO}), lowest unoccupied molecular orbital (E_{LUMO}), dipole moment, energy gap, electron affinity, ionization potential, electronegativity, global hardness, and softness (listed in Table 8), were found to influence the relationship between the molecular structure (CS surface) and its electron static dipole (ESD) [41]. The E_{HOMO} value of an inhibitor reflects its ability to donate electrons to the empty d-orbitals on the CS surface. A higher E_{HOMO} correlates with increased electron donation, which enhances the inhibitor's adsorption efficiency. Conversely, the E_{LUMO} value indicates the molecule's propensity to accept electrons. A lower E_{LUMO} suggests a greater ability to receive electrons". Since ΔE represents the energy required to remove an electron from the highest occupied orbital, a lower ΔE value is generally preferred:

$$\Delta E = E_{LUMO} - E_{HOMO} \qquad (10)$$

"Ionization potential (I) and electron affinity (A) are related to the highest occupied molecular orbital (E_{HOMO}) and lowest unoccupied molecular orbital (E_{LUMO}), respectively, highlighting the connection between these properties. Absolute electronegativity (χ) and hardness (η) are calculated using specific equations". The global softness (σ) of the inhibitor molecule can be determined using the following equations.

$$I = -E_{HOMO} \qquad (11)$$

$$A = -E_{LUMO} \qquad (12)$$

$$\chi = \frac{I+A}{2} = -\frac{E_{HOMO}+E_{LUMO}}{2} \qquad (13)$$

$$\eta = \frac{I-A}{2} = \frac{E_{LUMO}-E_{HOMO}}{2} = \frac{1}{2}\Delta E_{L-H} \qquad (14)$$

$$\sigma = \frac{1}{\eta} \qquad (15)$$

A lower global softness value enhances the reactivity and inhibition efficiency of the ESD. "A higher dipole moment promotes the adsorption of ESD onto the CS surface. The strong dipole-dipole interactions between the inhibitor and the metal surface, as shown Table 8, contribute to the high dipole moment of the inhibitor. Certain parameters, such as global hardness and softness, are related to the molecule's selectivity and reactivity". According to Lewis acid-base theory and Pearson's hard-soft acid-base theory, harder molecules with larger ΔE values tend to be more reactive [42].

	Neutral	Protonated
ilken structure	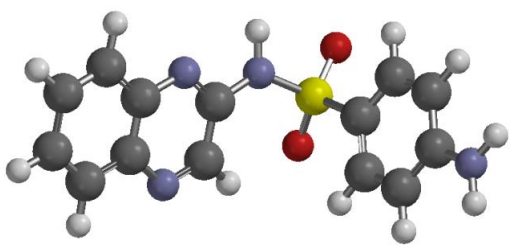	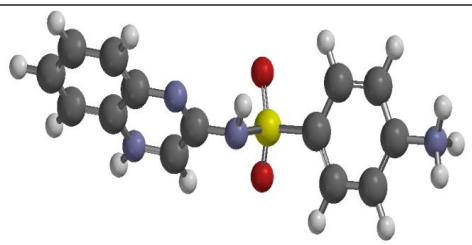
HOMO	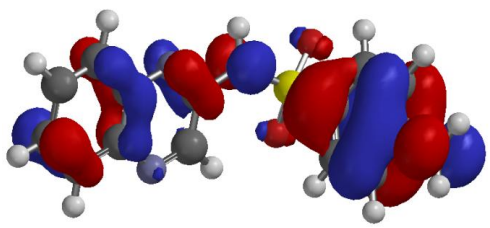	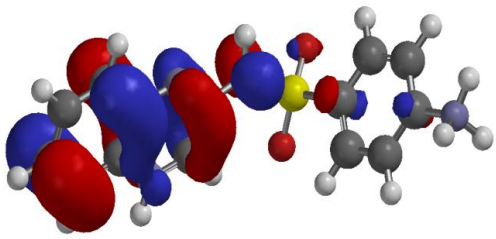
LUMO	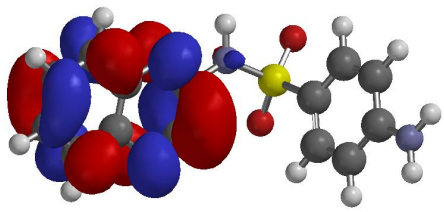	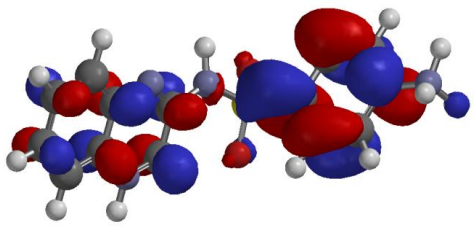

Fig. 13. "The frontier molecular provides the electron density maps of HOMO and LUMO for the EDD"

Table 8: "Quantum calculation parameters for molecule of EDD obtained from DFT"

Parameters (Variable)	DFT	
	Neutral	Protonated
$-E_{HOMO}$ (ev)	8.47	8.11
$-E_{LUMO}$ (ev)	1.97	2.21
ΔE, (eV) (E_L-E_H)	6.50	5.90
μ (debye) (Dipole moment)	7.51	9.47
A (eV) (electron affinity)	1.97	2.21
I (eV) (ionization potential)	8.47	8.11
χ (eV) (electronegativity)	5.22	5.16
η (eV) (global hardness)	3.25	2.95
ΔN	0.27	0.31
σ (eV^{-1}) (softness)	0.31	0.34

4. Inhibition mechanism

During the studying of WL and electrochemical measurements we noted that the corrosion of CS decreased by the addition of ESD. "The results of these measurements appeared that the inhibition mechanism depended on the adsorption ESD on CS surface which closed the active sites on it. The presence of chemical compounds such as (4-isopropylbenzaldehyde, β-Pinene, γ-terpinene , p -cymene) were detected by Photochemical analysis. These compounds contain heteroatoms (N, O) which adsorbed on the metal surface. This study detected that the adsorption is physical adsorption and the adsorbed molecule form a coated layer on CS to inhibit its corrosion [43-44]. The Cl^- ions get adsorbed on surface CS and turn it as negatively charged surface, the protonated ESD molecules (cationic) get adsorbed on the negatively charged surface of CS by an electrostatic attraction". The protonated molecules could adsorb on specimen CS surface Fig. 14.

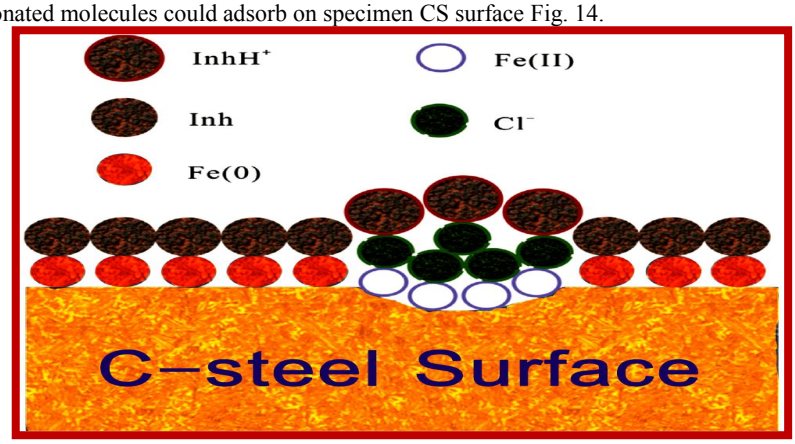

Fig. 14. The ESD in 1 M HCl solution are absorbed and inhibited dissolution of CS

5. Conclusions

With respect to the outcome data the next conclusions were recorded:

1. ESD is a fine green inhibitor that exhibits excellent inhibition efficiency against the corrosion of mild steel (MS) in acidic environments.
2. The inhibition efficiency (IE %) increased with both increasing ESD concentration and rising temperature.
3. Langmuir isotherm used to designate the ESD adsorbed of on CS surface.
4. Surface analysis was achieved by using (AFM, FT-IR and XPS).
5. The weight loss (WL) measurements were found to be in good agreement with the electrochemical tests.

References

[1] R.E. Melchers, Corrosion at the Steel–Medium Interface, Corros. Mater. Degrad. 5 (2024) 52–72.
[2] L. Herrag, B. Hammouti, S. Elkadiri, A. Aouniti, C. Jama, H. Vezin, F. Bentiss, Adsorption properties and inhibition of mild steel corrosion in hydrochloric solution by some newly synthesized diamine derivatives: experimental and theoretical investigations, Corros. Sci. 52 (2010) 3042–3051.
[3] E. Bayol, T. Gürten, A.A. Gürten, M. Erbil, Interactions of some Schiff base compounds with mild steel surface in hydrochloric acid solution, Mater. Chem. Phys. 112 (2008) 624–630.
[4] S. Cheng, S. Chen, T. Liu, X. Chang, Y. Yin, Carboxymethylchitosan+ Cu2+ mixture as an inhibitor used for mild steel in 1 M HCl, Electrochim. Acta. 52 (2007) 5932–5938.
[5] A. Fouda, M.A. Azeem, S. Mohamed, A. El-Desouky, Corrosion inhibition and adsorption behavior of nerium oleander extract on carbon steel in hydrochloric acid solution, Int J Electrochem Sci. 14 (2019) 3932–3948.
[6] D.D.N. Singh, A.K. Dey, Synergistic effects of inorganic and organic cations on inhibitive performance of propargyl alcohol on steel dissolution in boiling hydrochloric acid solution, Corrosion. 49 (1993) 594–600.
[7] G. Banerjee, S.N. Malhotra, Contribution to adsorption of aromatic amines on mild steel surface from HCl solutions by impedance, UV, and Raman spectroscopy, Corrosion. 48 (1992) 10–15.
[8] M.A. Migahed, E.M.S. Azzam, A.M. Al-Sabagh, Corrosion inhibition of mild steel in 1 M sulfuric acid solution using anionic surfactant, Mater. Chem. Phys. 85 (2004) 273–279.
[9] R.F. V Villamil, P. Corio, S.M.L. Agostinho, J.C. Rubim, Effect of sodium dodecylsulfate on copper corrosion in sulfuric acid media in the absence and presence of benzotriazole, J. Electroanal. Chem. 472 (1999) 112–119.
[10] S.S. Abd El Rehim, H.H. Hassan, M.A. Amin, The corrosion inhibition study of sodium dodecyl benzene sulphonate to aluminium and its alloys in 1.0 M HCl solution, Mater. Chem. Phys. 78 (2003) 337–348.
[11] R. Guo, T. Liu, X. Wei, Effects of SDS and some alcohols on the inhibition efficiency of corrosion for nickel, Colloids Surfaces A Physicochem. Eng. Asp. 209 (2002) 37–45.
[12] V. Branzoi, F. Golgovici, F. Branzoi, Aluminium corrosion in hydrochloric acid solutions and the effect of some organic inhibitors, Mater. Chem. Phys. 78 (2003) 122–131.
[13] R. Oukhrib, B. El Ibrahimi, H. Bourzi, K. El Mouaden, A. Jmiai, S. El Issami, L. Bammou, L. Bazzi, Quantum chemical calculations and corrosion inhibition efficiency of biopolymer "chitosan" on copper surface in 3% NaCl, J. Mater. Environ. Sci. 8 (2017) 195–208.
[14] A.M. Al-Azzawi, K.K. Hammud, newly antibacterial/anti-rusting oxadiazole poromellitic di-imids of carbon steel/hydrochloric acid interface: Temkin isother model, IJRPC. 6 (2016) 391–402.
[15] H. Oudda, F. El-Hajjaji, B. Hammouti, Synthesis and inhibition study of carbon steel corrosion in hydrochloric acid of a new surfactant derived from 2-mercaptobenzimidazole, (n.d.).
[16] U.M. Sani, U. Usman, Electrochemical corrosion inhibition of mild steel in hydrochloric acid medium using the antidiabetic drug janumet as inhibitor, Int. J. Nov. Res. Phy. Chem. Math. 3 (2016) 30–37.
[17] A.M. Kolo, U.M. Sani, U. Kutama, U. Usman, Adsorption and Inhibitive properties of januvia for the corrosion of Zn in 0.1 M HCl, Pharm. Chem. J. 3 (2016) 109–119.
[18] P.O. Ameh, N.O. Eddy, Commiphora pedunculata gum as a green inhibitor for the corrosion of aluminium alloy in 0.1 M HCl, Res. Chem. Intermed. 40 (2014) 2641–2649.
[19] H.I. Al-Shafey, R.S.A. Hameed, F.A. Ali, A.E.-A.S. Aboul-Magd, M. Salah, Effect of expired drugs as corrosion inhibitors for carbon steel in 1M HCL solution, Int. J. Pharm. Sci. Rev. Res. 27 (2014) 146–152.
[20] R. Kushwah, R.K. Pathak, Inhibition of mild steel corrosion in 0.5 M sulphuric acid solution by aspirin drug, Int. J. Emerg. Technol. Adv. Eng. 4 (2014) 880–884.
[21] A.S. Fouda, M.N. El-Haddad, Y.M. Abdallah, Septazole: antibacterial drug as a green corrosion inhibitor for copper in hydrochloric acid solutions, Int. J. Innov. Res. Sci. Eng. Technol. 2 (2013) 7073–7085.
[22] S.U. Ofoegbu, P.U. Ofoegbu, Corrosion inhibition of mild steel in 0.1 M hydrochloric acid media by chloroquine diphosphate, ARPN J. Eng. Appl. Sci. 7 (2012) 272–276.
[23] A. Ovung, J. Bhattacharyya, Sulfonamide drugs: Structure, antibacterial property, toxicity, and biophysical interactions, Biophys. Rev. 13 (2021) 259–272.
[24] D.A. Shifler, D.G. Enos, Marine Corrosion Testing, LaQue's Handb. Mar. Corros. (2022) 379–420.
[25] E. Cano, J.L. Polo, A. La Iglesia, J.M. Bastidas, A study on the adsorption of benzotriazole on copper in hydrochloric acid using the inflection point of the isotherm, Adsorption. 10 (2004) 219–225.
[26] L. Narvaez, E. Cano, D.M. Bastidas, 3-Hydroxybenzoic acid as AISI 316L stainless steel corrosion inhibitor in a H 2 SO 4–HF–H 2 O 2 pickling solution, J. Appl. Electrochem. 35 (2005) 499–506.
[27] A.E.-A.S. Fouda, S.E.H. Etaiw, D.M. Abd El-Aziz, A.A. El-Hossiany, U.A. Elbaz, Experimental and theoretical studies of the efficiency of metal–organic frameworks (MOFs) in preventing aluminum corrosion in hydrochloric acid solution, BMC Chem. 18 (2024) 21.
[28] H.A. Ali, A.A. El-Hossiany, A.S. Abousalem, M.A. Ismail, A.E.-A.S. Fouda, E.A. Ghaith, Synthesis of new binary trimethoxyphenylfuran pyrimidinones as proficient and sustainable corrosion inhibitors for carbon steel in acidic medium: experimental, surface morphology analysis, and theoretical studies, BMC Chem. 18 (2024) 182.
[29] M.M. Saleh, A.A. Atia, Effects of structure of the ionic head of cationic surfactant on its inhibition of acid corrosion of mild steel, J. Appl. Electrochem. 36 (2006) 899–905.
[30] K. Rose, B.-S. Kim, K. Rajagopal, S. Arumugam, K. Devarayan, Surface protection of steel in acid medium by Tabernaemontana divaricata extract: physicochemical evidence for adsorption of inhibitor, J. Mol. Liq. 214 (2016) 111–

116.
[31] A.E.-A.S. Fouda, A.F. Molouk, M.F. Atia, A. El-Hossiany, M.S. Almahdy, Verbena officinalis (VO) leaf extract as an anti-corrosion inhibitor for carbon steel in acidic environment, Sci. Rep. 14 (2024) 16112.
[32] Y. Zhu, M.L. Free, G. Yi, Experimental investigation and modeling of the performance of pure and mixed surfactant inhibitors: aggregation, adsorption, and corrosion inhibition on steel pipe in aqueous phase, J. Electrochem. Soc. 162 (2015) C582.
[33] A. Zarei, A. Dehghani, L. Guo, B. Ramezanzadeh, Pepper extract effectiveness as a natural inhibitor against corrosion of steel samples (SS) in 1 M hydrochloric acid; Theoretical (DFT calculation–MD simulation), thermodynamic, and electrochemical-surface studies, Ind. Crops Prod. 189 (2022) 115839.
[34] M.M. Saleh, M.G. Mahmoud, H.M. Abd El-Lateef, Comparative study of synergistic inhibition of mild steel and pure iron by 1-hexadecylpyridinium chloride and bromide ions, Corros. Sci. 154 (2019) 70–79.
[35] A.S. Fouda, S. Rashwaan, H. Ibrahim, R.E. Ahmed, Corrosion inhibition of α-brass alloy in aqueous solution by using expired Ranitidine, Int. J. Electrochem. Sci. 15 (2020) 5982–6000.
[36] S.F. Abd El Aziz, S.E.H. Etaiw, S. Sobhy, Metal-organic frameworks based on heterocyclic ligands and some transition metals as effective carbon steel corrosion inhibitors in aqueous environment, J. Mol. Liq. 348 (2022) 118402.
[37] A.S. Fouda, M. Eissa, A. El-Hossiany, Ciprofloxacin as eco-friendly corrosion inhibitor for carbon steel in hydrochloric acid solution, Int. J. Electrochem. Sci. 13 (2018) 11096–11112. https://doi.org/10.20964/2018.11.86.
[38] M.A. Abd El-Ghaffar, M.H. Sherif, A. Taher El-Habab, Synthesis, characterization, and evaluation of ethoxylated lauryl-myrisityl alcohol nonionic surfactants as wetting agents, anti-foamers, and minimum film forming temperature reducers in emulsion polymer lattices, J. Surfactants Deterg. 20 (2017) 117–128.
[39] X. Wang, Y. Pan, J. Yang, R. Zhu, Y. Zhou, Z. Yuan, H. Chu, P. Hu, L. Li, Corrosion behavior of Ti-0.3 Mo-0.8 Ni (TA10) alloy in proton exchange membrane fuel cell environment: Experimental and theoretical studies, Int. J. Electrochem. Sci. 18 (2023) 100239.
[40] A.S. Fouda, S.A. Abd El-Maksoud, A. El-Hossiany, A. Ibrahim, Corrosion protection of stainless steel 201 in acidic media using novel hydrazine derivatives as corrosion inhibitors, Int. J. Electrochem. Sci. 14 (2019) 2187–2207.
[41] F. Benhiba, Z. Benzekri, Y. Kerroum, N. Timoudan, R. Hsissou, A. Guenbour, M. Belfaquir, S. Boukhris, A. Bellaouchou, H. Oudda, Assessment of inhibitory behavior of ethyl 5-cyano-4-(furan-2-yl)-2-methyl-6-oxo-1, 4, 5, 6-tetrahydropyridine-3-carboxylate as a corrosion inhibitor for carbon steel in molar HCl: Theoretical approaches and experimental investigation, J. Indian Chem. Soc. 100 (2023) 100916.
[42] D.M. Jamil, A.K. Al-Okbi, S.B. Al-Baghdadi, A.A. Al-Amiery, A. Kadhim, T.S. Gaaz, A.A.H. Kadhum, A.B. Mohamad, Experimental and theoretical studies of Schiff bases as corrosion inhibitors, Chem. Cent. J. 12 (2018) 1–9.
[43] A.S. Fouda, S.A. Abd El-Maksoud, A. El-Hossiany, A. Ibrahim, Evolution of the corrosion-inhibiting efficiency of novel hydrazine derivatives against corrosion of stainless steel 201 in acidic medium, Int. J. Electrochem. Sci. 14 (2019) 6045–6064.
[44] A. Habibiyan, B. Ramezanzadeh, M. Mahdavian, M. Kasaeian, Facile size and chemistry-controlled synthesis of mussel-inspired bio-polymers based on Polydopamine Nanospheres: application as eco-friendly corrosion inhibitors for mild steel against aqueous acidic solution, J. Mol. Liq. 298 (2020) 111974.